

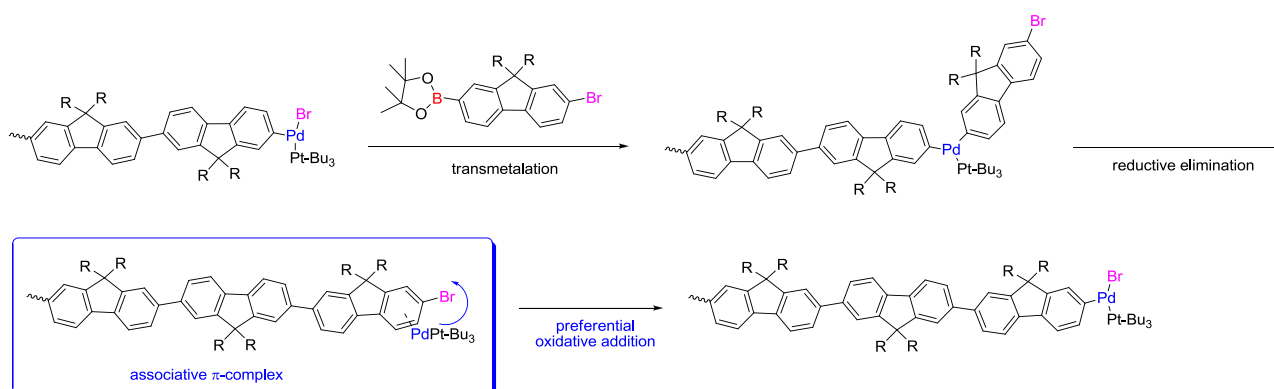
# **Impact of Precatalyst Activation in Suzuki-Miyaura Catalyst-Transfer Polymerizations: New Mechanistic Scenarios for Pre-Transmetalation Events**

*Roberto Grisorio\* and Gian Paolo Suranna*

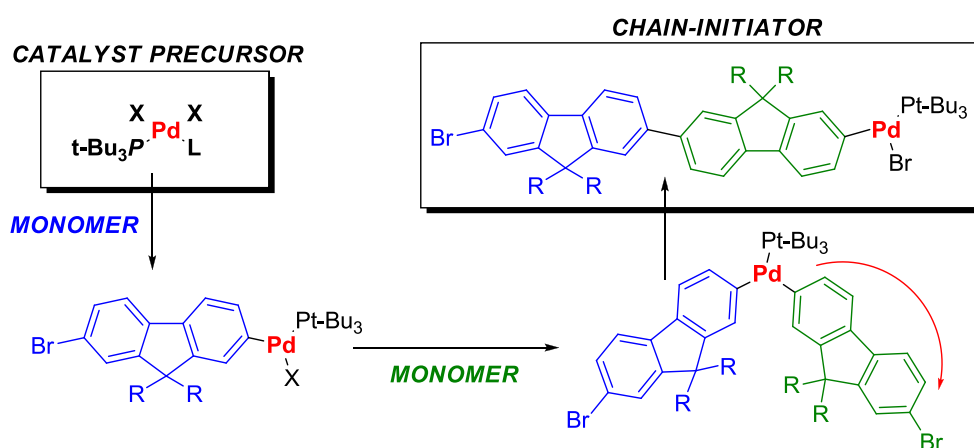
*DICATECh - Dipartimento di Ingegneria Civile, Ambientale, del Territorio, Edile e di Chimica, Via Orabona, 4 I-70125 Bari, Italy and CNR-NANOTEC – Istituto di Nanotecnologia, Polo di Nanotecnologia c/o Campus Ecotekne, via Monteroni, 73100 Lecce, Italy.*

**General remarks:** 2,7-dibromo-9,9-di-*n*-octylfluorene<sup>1</sup> and 2-(7-bromo-9,9-di-*n*-octyl-fluoren-2-yl)-4,4,5,5-tetramethyl-1,3,2-dioxaborolane<sup>2</sup> were synthesized according to literature procedures. Tri-(*t*-butyl)phosphane, palladium(II) sources and the employed bases were purchased from standard commercial sources and used as received. All solvents used were carefully dried and freshly distilled according to standard laboratory practice. All manipulations were carried out under inert nitrogen atmosphere using common Schlenk techniques. Flash chromatography was performed using a silica gel of 230-400 mesh. NMR spectra were recorded on a Bruker Avance 700 MHz instrument. Gel Permeation Chromatography (GPC) analyses were carried out on an Agilent Series 1100 instrument equipped with a PL-gel 5  $\mu$ m mixed-C column. THF solutions for GPC analysis were eluted at 25 °C at a flow rate of 1.0 mL/min and analyzed using a multiple wave UV-Vis detector. Number-average molecular weights ( $M_n$ ), weight-average molecular weights ( $M_w$ ) and polydispersity indexes (PDI) are relative to polystyrene standards.

**Computational Details:** All stationary points were fully optimized at the DFT level with the hybrid B3LYP functional as implemented in the Gaussian09 software package (Rev. D.01).<sup>3</sup> Geometry optimizations were carried out on the full system without including solvation. Frequencies were computed with the aim of classifying all stationary points as minima (reactants, intermediates and products, with all real frequencies). These calculations were also used to determine the thermochemistry corrections, which include the zero-point energies, thermal contributions and entropies. The basis sets combine the 6-311G+(d,p) (C, N, O, P, B, Cl and H) and the LANL2DZ (Pd) basis sets using M06 and PBE0 functionals. Transition states were identified by having one imaginary frequency in the Hessian matrix.



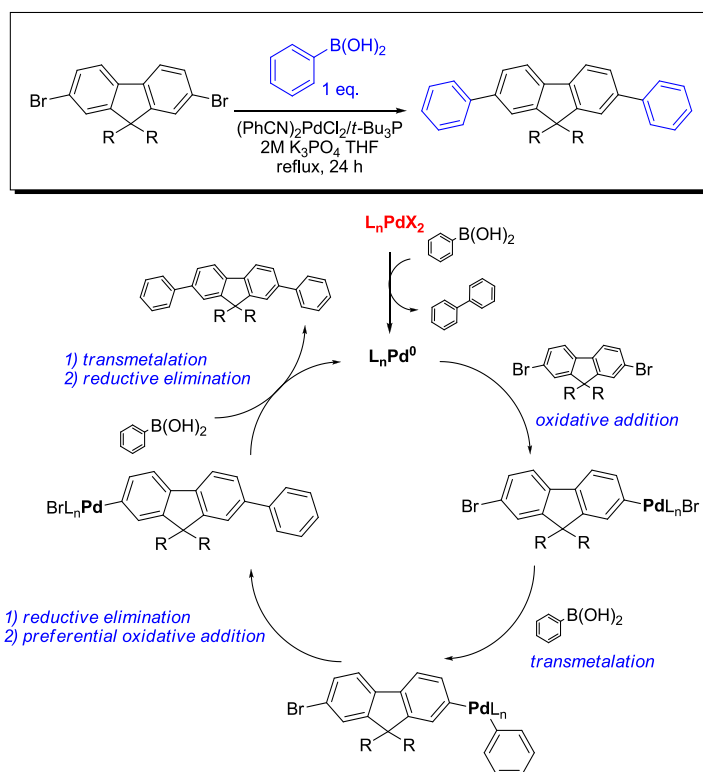
**Scheme S1.** Intramolecular catalyst-transfer process (reductive elimination/associative  $\pi$ -complex/preferential oxidative addition) for a fluorene-based AB-type monomer chain-growth polymerization.



**Scheme S2.** Postulated initiation step of the chain-growth polymerization employing  $L_2PdX_2$  as the  $Pd^{II}$  precatalyst ( $L = PhCN$ ,  $CH_3CN$  or  $Cl^-$ ) in the presence of  $tBu_3P$  as the external ligand. The traditional role of  $tBu_3P$  ligand has been considered (neutral pathway).

## Model reaction

In order to ascertain whether  $L_nPdX_2$  precatalysts can provide an effective precursor for chain-growth polymerizations, the necessary model reaction between 2,7-dibromo-9,9-di-*n*-octylfluorene and an equimolar amount of phenyl-boronic acid using  $(PhCN)_2PdCl_2/t-Bu_3P$  as the catalytic system was appropriately set up. The use of a sub-stoichiometric amount of phenyl-boronic acid with respect to the dibromo-derivative substantiates the "preferential oxidative addition pathway" (the mandatory prerequisite for the actuation of a chain-growth polymerization) from the simple product distribution.<sup>4</sup> The negligible formation of the mono-substituted product confirms that the reductive elimination of the Suzuki cross-coupling yields a palladium species remaining associated with the formed product, with the subsequent activation of the remaining C–Br bond (Scheme S3). This results confirms that a preferential oxidative addition takes place, which is the key requisite for the insurgence of a chain-growth pathway (*i.e.* the propagation stage) in the polymerization (*vide infra*).



**Scheme S3.** Top: reaction between 2,7-dibromo-9,9-di-*n*-octylfluorene and phenyl-boronic acid (1.0 equiv) using  $Pd^{II}$  sources as the catalyst precursors. Bottom: reaction pathway for the selective obtainment of the di-substituted fluorene derivative on the basis of the propagation stage in chain-growth polymerizations.

**Experimental section:** A mixture of (PhCN)<sub>2</sub>PdCl<sub>2</sub> (3.4 mg,  $1.5 \times 10^{-2}$  mmol) and *t*-Bu<sub>3</sub>P (2.0 equiv with respect to Pd) in THF (3.0 mL) was kept under stirring for 5 min at room temperature. Then, the addition of phenyl-boronic acid (61.0 mg, 0.50 mmol), 2,7-dibromo-9,9-di-*n*-octylfluorene (0.274 g, 0.50 mmol) and potassium phosphate (0.318 g, 1.50 mmol) was performed. The resulting mixture was kept at 70 °C for 24 h. The reaction flask was cooled down to room temperature and methylene chloride (50 mL) was added. The obtained mixture was washed with water (50 mL) and the organic phase was dried over sodium sulphate. The solvent was removed *in vacuo* and the crude product was purified by column chromatography (SiO<sub>2</sub>, petroleum ether 40-60 °C → petroleum ether 40-60 °C/CH<sub>2</sub>Cl<sub>2</sub> = 9/1) yielding 2,7-diphenyl-9,9-di-*n*-octylfluorene<sup>4</sup> and the unreacted substrate (2,7-dibromo-9,9-di-*n*-octylfluorene).

### Polymerization reaction

**Typical reaction conditions (entry 3):** A solution of 2-(7-bromo-9,9-di-*n*-octyl-fluoren-2-yl)-4,4,5,5-tetramethyl-1,3,2-dioxaborolane (59.6 mg, 0.10 mmol), Na<sub>2</sub>PdCl<sub>4</sub> (5% mol/mol, 1.5 mg,  $0.5 \times 10^{-2}$  mmol) and *t*-Bu<sub>3</sub>P (2.0 mg,  $1.0 \times 10^{-2}$  mmol) in THF (5 mL) was kept under stirring for 5 min at room temperature (forming a yellow solution) before the addition of a 2 M K<sub>3</sub>PO<sub>4</sub> aqueous solution (0.5 mL) which initiated the polymerization. The resulting mixture was stirred at room temperature for 30 min and then quenched by pouring it into a beaker containing methanol (150 mL) and an aqueous HCl solution (1 N, 15 mL). The polymer precipitated was collected by centrifugation, washed with petroleum ether 40-60 °C to remove monomer traces, and eventually dried *in vacuo* for 24 h. The polymer was isolated as a pale yellow solid. The end-group analysis of the polyfluorenes obtained in this investigation was carried out by <sup>1</sup>H-NMR spectroscopy. In the <sup>1</sup>H-NMR spectra (see figure S1) the signals at 7.3–7.4 ppm are assigned to the protons of the H-termination, while the signals at 7.5–7.6 ppm suggest that Br-terminations are present in the synthesized polymers,<sup>5</sup> strongly supporting an H/Br termination of the macromolecules.

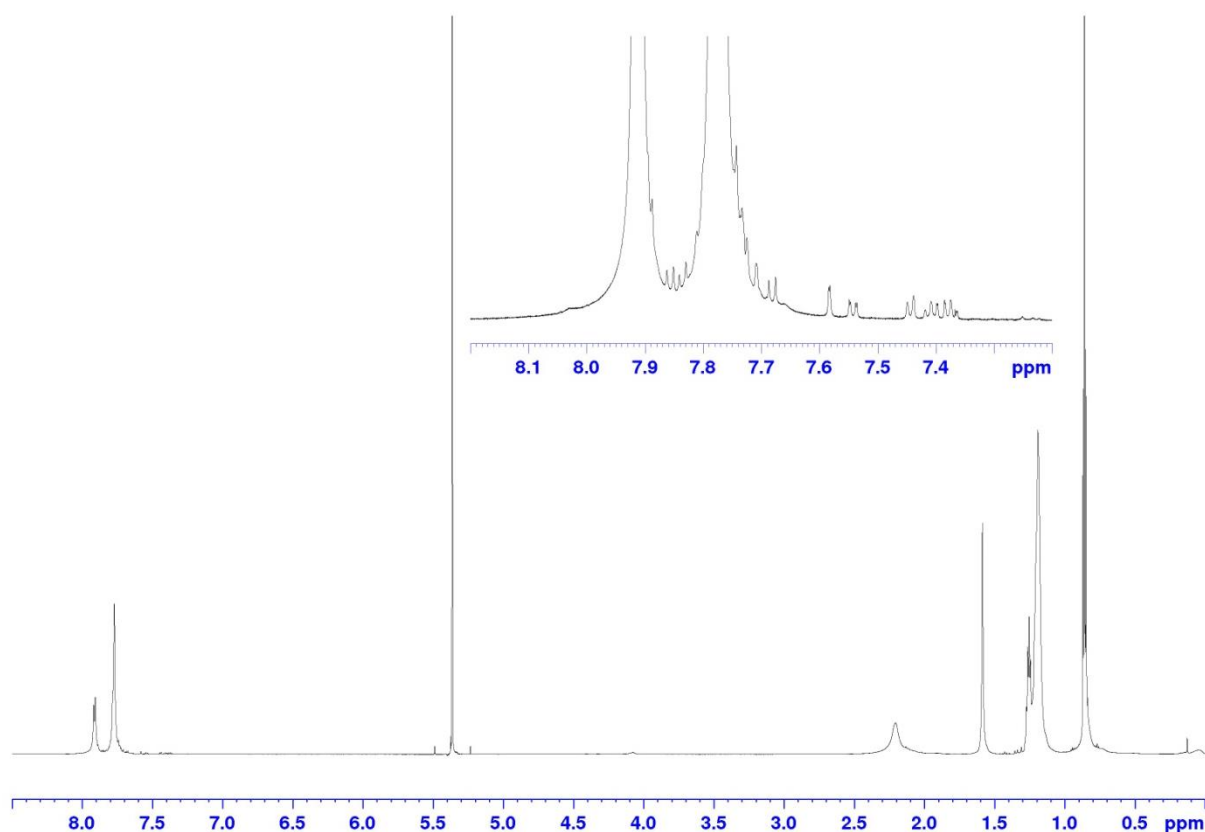


**Figure S1.**  $^1\text{H}$ -NMR spectrum ( $\text{CD}_2\text{Cl}_2$ ) of the poly(fluorene) obtained from the reaction in entry 3.

### Polymerization monitoring

For the monitoring of the number-average molecular weights ( $M_n$ ) of the forming polymer as function of the monomer conversion, the polymerization reaction was repeated by following the procedure described for entry 3 except for the presence of fluorene (40.0 mg) as the internal standard. Small aliquots of the reaction mixture were sampled at intervals of 3 min and were poured into methanol, causing the polymer precipitation. In order to evaluate the monomer conversion, after the necessary centrifugation, the supernatant solutions were analysed by GPC, while the insoluble polymer was dissolved in THF and analyzed by GPC. The  $M_n$  (PDI) values after 34%, 42%, 53%, 65%, 74%, 83%, 92% and 100% monomer conversion were found to be 7000 (1.46), 9500 (1.45), 12100 (1.48), 16200 (1.51), 18500 (1.49), 21400 (1.50), 24200 (1.50) and 26400 (1.51) Da, respectively. The linear behaviour of  $M_n$  vs monomer conversion (Figure S2) is strongly indicative of the onset of a chain-growth regime for the polymerization course.

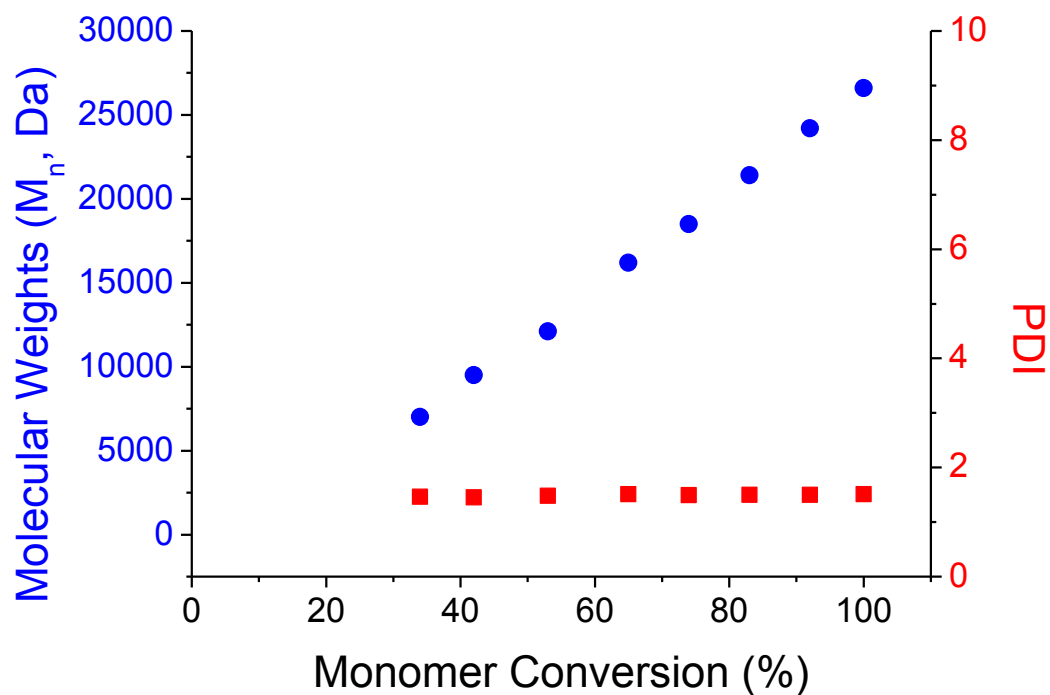
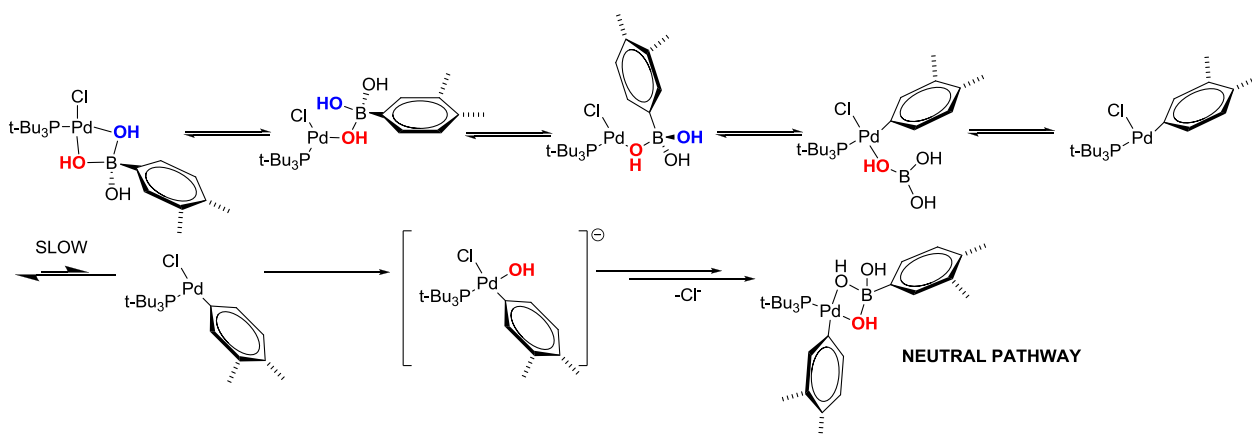


**Figure S2.** Number-average molecular weights ( $M_n$ ) of the forming polymer as a function of monomer conversion (polymerization conditions of entry 3).



**Scheme S4.** Alleged reaction steps for the precatalyst activation after the first transmetalation event, which lead to a species having an open coordination site, which hampers the transmetalation event upon addition of the hydroxide group to the complex. The slow isomerization of this species can afford a T-shaped complex favoring the neutral pathway.

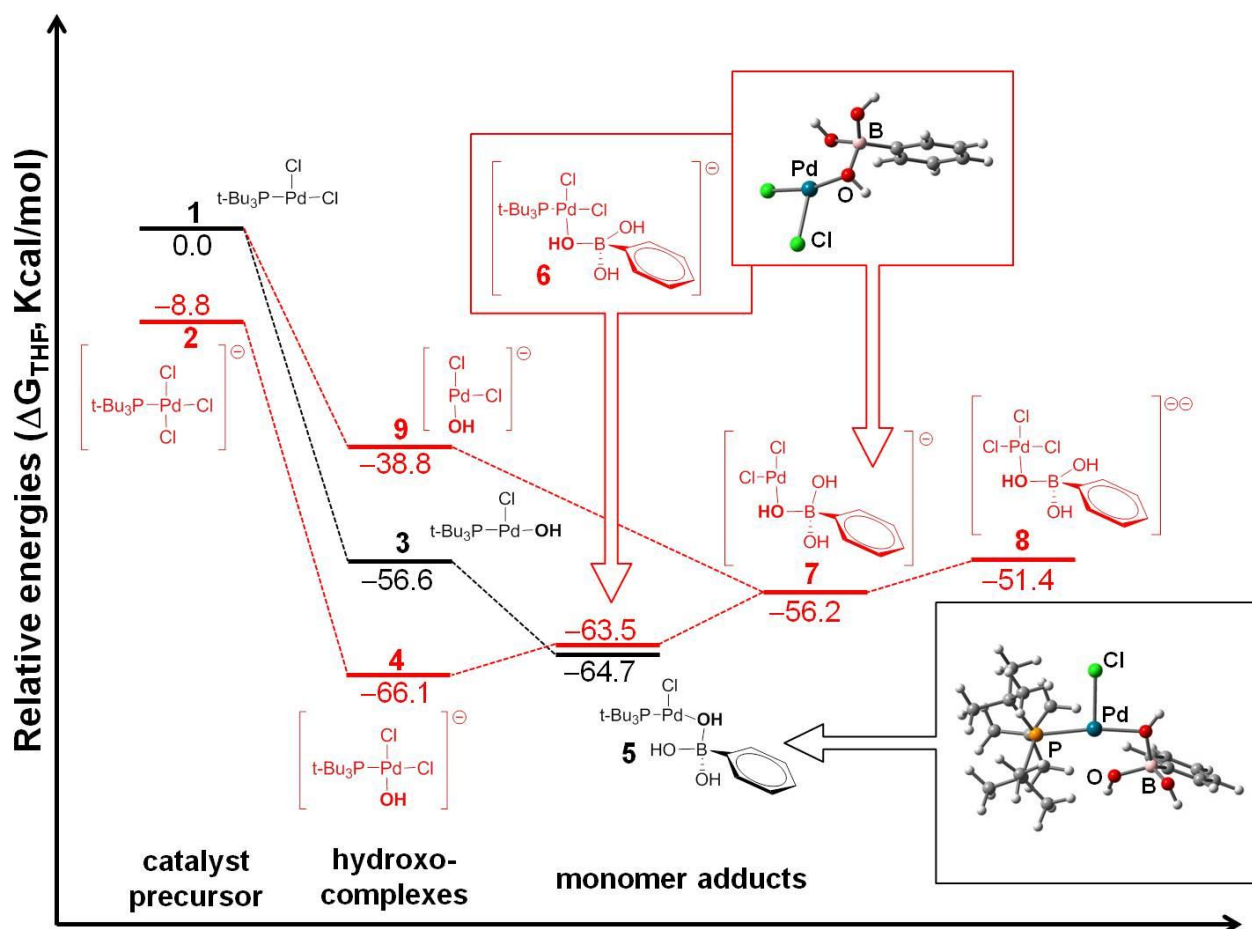


**Figure S3.** DFT energy profile (Kcal/mol) for the steps anticipating the first transmetalation formally employing  $\text{PdCl}_2$  or  $\text{PdCl}_4^{2-}$  in the presence of  $t\text{-Bu}_3\text{P}$  as the external ligand and phenyl boronic acid (no cation). Free energies (Kcal/mol) are calculated using M06/LANL2DZ-6-311G+(d,p) with CPCM solvation modeling (THF). Insets: geometrically optimized structures for the monomer adducts **5** and **7** in the case of the neutral (black trace) and anionic (red trace) pathway, respectively. For clarity, the energy levels are not exactly scaled.

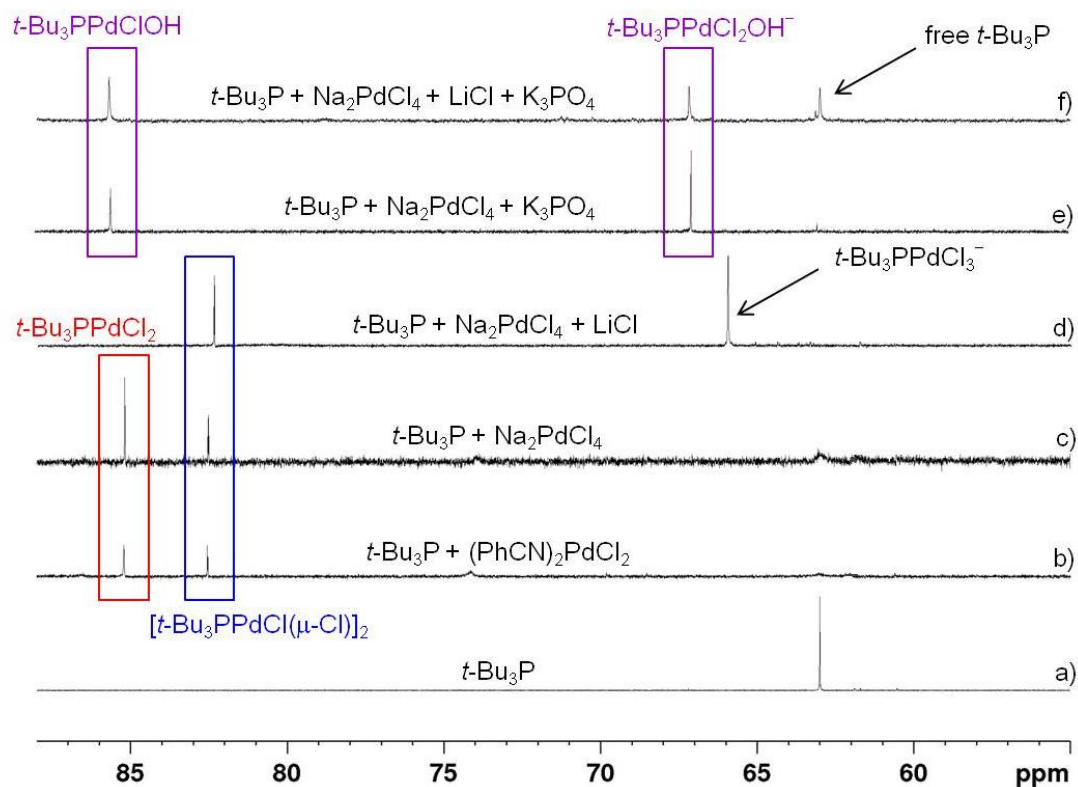


**Figure S4.**  $^{31}\text{P}$ -NMR spectra of a)  $t\text{-Bu}_3\text{P}$ , b)  $t\text{-Bu}_3\text{P}/(\text{PhCN})_2\text{PdCl}_2$ , c)  $t\text{-Bu}_3\text{P}/\text{Na}_2\text{PdCl}_4$  and d)  $t\text{-Bu}_3\text{P}/\text{Na}_2\text{PdCl}_4/\text{LiCl}$  recorded in  $\text{THF-d}_8$ . The spectra e) and f) were recorded after addition of a 2M  $\text{K}_3\text{PO}_4$  aqueous solution ( $\text{D}_2\text{O}$ ) to the mixture described by spectra c) and d), respectively. The  $\text{THF-d}_8/\text{D}_2\text{O}$  ratio is the same of the polymerization reactions. Due to the immiscibility of  $\text{THF-d}_8$  with the 2M  $\text{K}_3\text{PO}_4$  aqueous solution, only the organic phase in the NMR tube was sampled.



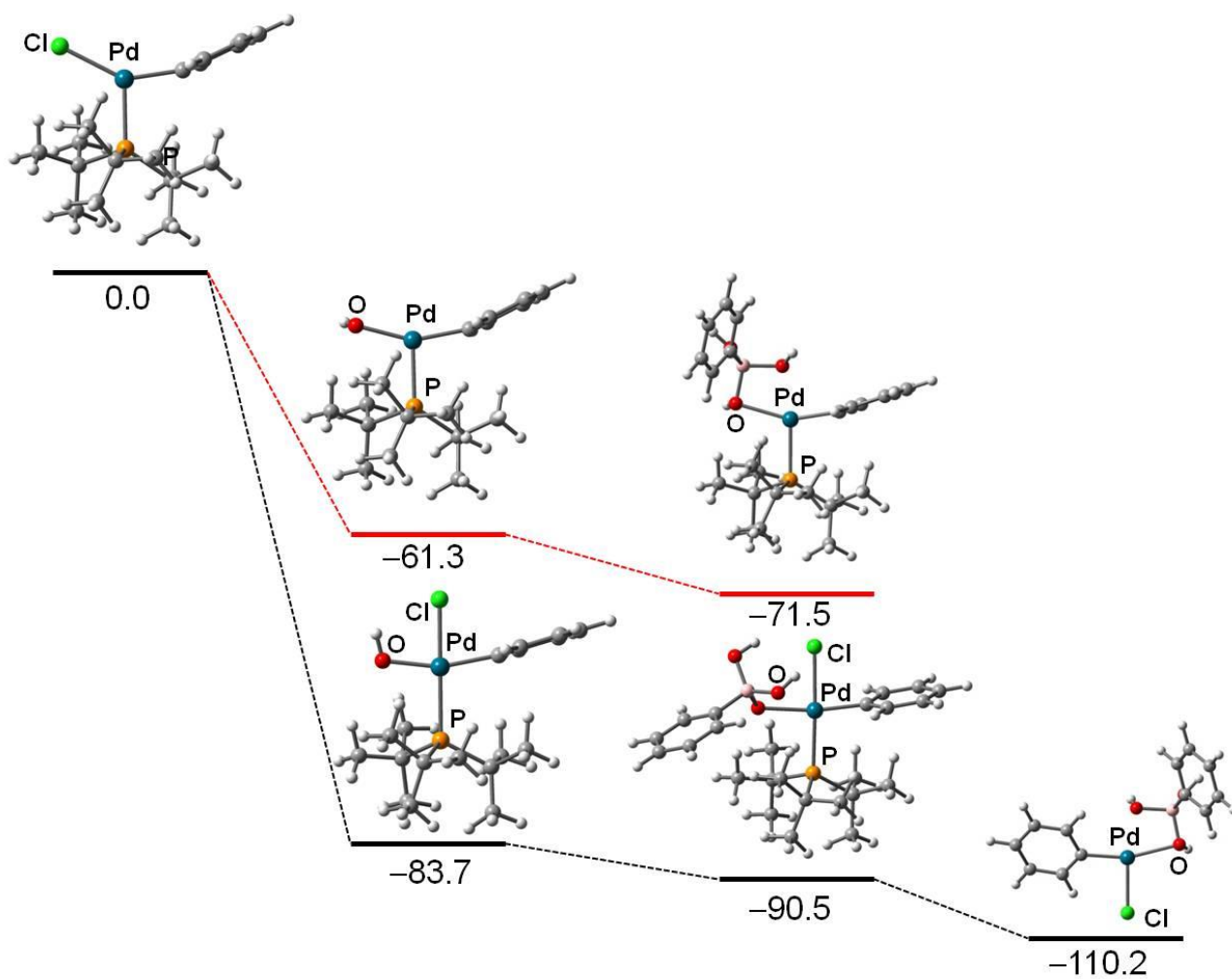


**Figure S5.** DFT energy profile (Kcal/mol) for the first transmetalation event in the case of the neutral (red trace) and anionic (black trace) pathways calculated using B3LYP/LANL2DZ-6-31G(d,p).

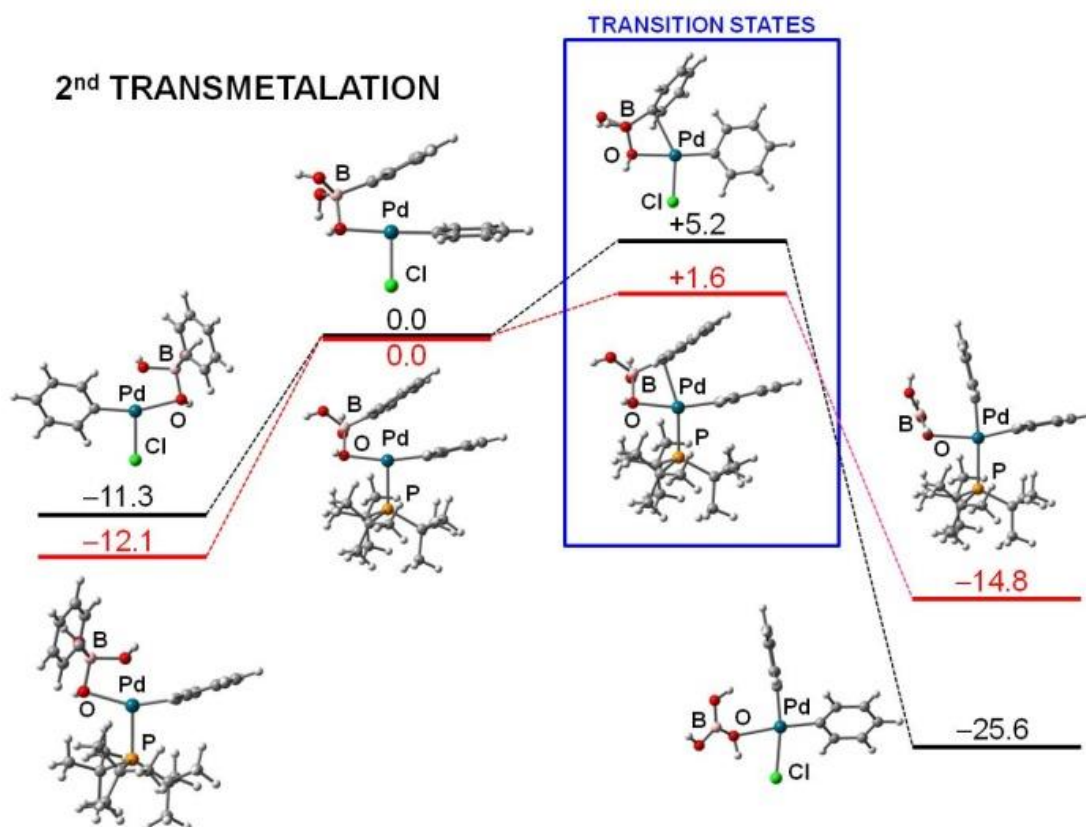
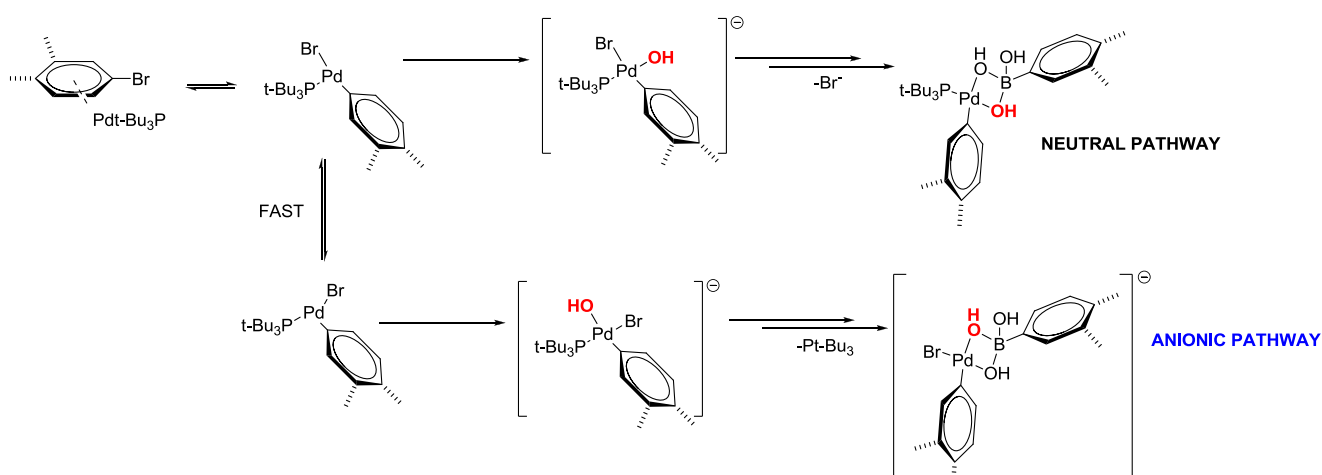


**Figure S6.** Normalized DFT energy profile (Kcal/mol) for the second transmetalation event in the case of the neutral (red trace) and anionic (black trace) pathways using B3LYP/LANL2DZ-6-31G(d,p).



**Scheme S5.** Alleged reaction steps for the propagation stage of the polymerization. The oxidative addition of the palladium centre to the C-Br bond leads to two T-shaped complexes, which can favor the neutral (top) or the anionic (bottom) pathway. In the absence of bromide excess, the neutral pathway is favored

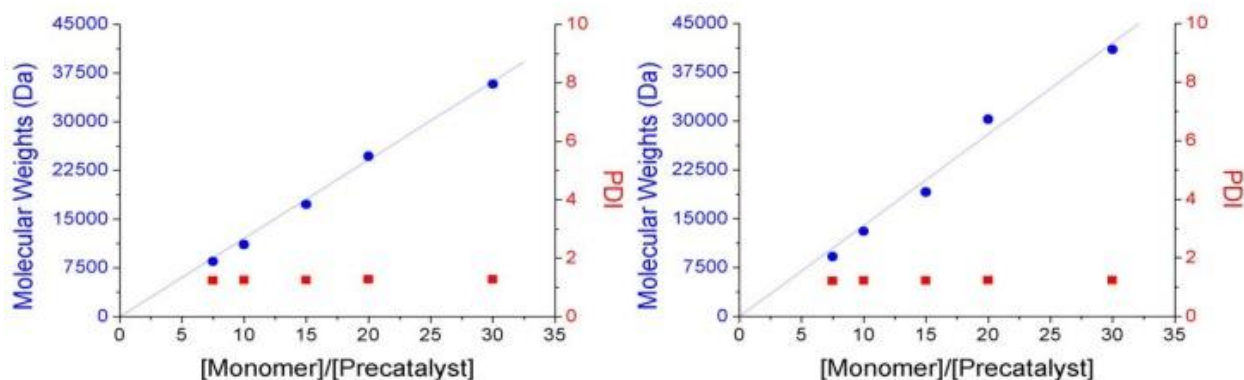


**Figure S7.** Molecular weights as a function of monomer/precatalyst molar ratio for polymerizations reported as entry 5 (left) and entry 11 (right) of Table 1 of the main text.

## References

- [1] Grisorio, R.; Mastroianni, P.; Nobile, C. F.; Romanazzi, G.; Suranna, G. P.; Gigli, G.; Piliego, C.; Ciccarella, G.; Cosma, P.; Acierno, D.; Amendola, E. *Macromolecules* **2007**, *40*, 4865–4873.
- [2] Yokoyama, A.; Suzuki, H.; Kubota, Y.; Ohuchi, K.; Higashimura, H.; Yokozawa, T. *J. Am. Chem. Soc.* **2007**, *129*, 7236–7237.
- [3] Frisch, M. J. *et al.* Gaussian09W, revision D.01, Gaussian, Inc., Wallingford CT, 2009.
- [4] (a) Groombridge, B. J.; Goldup, S. M.; Larrosa, I. *Chem. Commun.* **2015**, *51*, 3832–3834. (b) Larrosa, I.; Somoza, C.; Banquy, A.; Goldup, S. M. *Org. Lett.* **2011**, *13*, 146–149. (c) Dong, C.-G.; Hu, Q.-S. *J. Am. Chem. Soc.* **2005**, *127*, 10006–10007. For the limitations of the use of small molecules in order to identify catalyst-transfer reactions see: Bryan, Z. J.; Hall, A. O.; Zhao, C. T.; Chen, J.; McNeil, A. J. *ACS Macro Lett.* **2016**, *5*, 69–72.
- [5] Huang, L.; Wu, S.; Qu, Y.; Geng, Y.; Wang, F. *Macromolecules* **2008**, *41*, 8944–8947.